Int. J. Corros. Scale Inhib., 2013, **2**, no. 1, 67–81

Effect of molybdenum and tungsten polyoxometalates on the composition of surface layers and electrochemical behavior of stainless steel in sulfuric acid

L. P. Kazansky,* Yu. E. Pronin, E. M. Sokolova and S. S. Veselyi

A. N. Frumkin Institute of Physical Chemistry and Electrochemistry, Russian Academy of Sciences, Leninskii pr. 31, Moscow, 119071 Russian Federation
**E-mail: leoka@ipc.rssi.ru*

Abstract

The composition and thickness of the surface layers formed on ferrite steel at various applied potentials in pure 1 N H_2SO_4 and in the presence of polyoxometalate (POM) anions ($PMo_{12}O_{40}^{3-}$, $Mo_8O_{26}^{4-}$, and $PW_{12}O_{40}^{3-}$) have been studied by XPS. Noticeable changes in cationic composition are observed near the passivation potential. At anodic potentials the surface oxide layer is enriched by chromium oxide. The thickness of this layer does not exceed 2–3 nm. If polymolybdate or polytungstate anions are added to sulfuric acid, they are located mostly in the uppermost oxide layer. The anodic currents decrease notably with an increase in POM concentration. At the passivation potential the oxide layer thickness exceeds 3–4 nm and it is substantially enriched by molybdenum. On the samples kept for 1 h in 1 N H_2SO_4, a protective layer is formed in the presence of POM and an after-affect is achieved. This layer remains stable upon transfer into pure 1 N H_2SO_4, especially in the case of $PMo_{12}O_{40}^{3-}$. The stronger protective properties of $PMo_{12}O_{40}^{3-}$ are assumed to be due to its redox properties.

Key words: *stainless steel, passivation, surface layers, molybdenum and tungsten polyoxometalates, XPS study.*

Received: February 16, 2013 doi: 10.17675/2305-6894-2013-2-1-067-081

Introduction

Steel is an extremely important industrial material widely used in various areas, from large metal structures to the smallest surgical tools. The properties of a metal surface define its ability to withstand erosion and corrosion, and also define adhesion, wettability, biocompatibility, *etc*. Despite the high rust resistance of stainless steels (SS), their use in various corrosive atmospheres demands application of corrosion inhibitors such as oxoanions, in particular molybdate (MoO_4^{2-}) [1]. Molybdates are promising corrosion inhibitors, which in many cases can replace rather toxic chromates used as corrosion inhibitors for ferroalloys. They can be used by themselves [2–7] or in various mixtures [8]. On the other hand, molybdate does not possess such high oxidizing ability as CrO_4^{2-} that would favor to active formation of a protective oxide layer, hence it is a passivating inhibitor

also possessing ability to strengthen iron resistance to pitting [9]. Unlike CrO_4^{2-}, molybdate is not reduced on steel surfaces but forms iron molybdates, possibly having low solubility [10]. However, various polymolybdates and heteropolymolybdates (jointly referred to as polyoxometalates, or POM) having rather complex structures in acidic solutions possess high stability and oxidizing capability. Brasher [11] pointed out at the possibility of metal inhibition with phosphomolybdic acid $H_3PMo_{12}O_{40}$ (PMo_{12}) in neutral media, though it is known that in such media PMo_{12} partially decomposes and, most likely, as molybdate, favorably affects the corrosion behavior of metals. On the other hand, Lizlovs [12] investigated the influence of PMo_{12} addition on the electrochemical behavior of SS in sulfuric acid. Results of XPS studies have shown that phosphomolybdate anions are adsorbed in the surface oxide layer of SS samples exposed to 0.5 M and 0.005 M H_2SO_4 [13, 14]. The effect of phosphovanadomolybdates on the electrochemical behavior of mild steel was studied in neutral media [15]. An appreciable protective effect of polyoxotungstates in high-temperature water used in aluminum heat exchangers has been shown [16].

POMs adsorbed on the surfaces of noble metals were shown to form self-assembled ordered monomolecular layers [17–20], thus modifying the surface of metals and sometimes revealing unusual properties that can be useful in various areas of practical application [21, 22], particularly in corrosion protection [23].

This study deals with the electrochemical behavior of stainless steel (SS, an analog of steel 430) electrodes in 1 N H_2SO_4 in the presence of POM. Besides, the composition and thickness of the layers formed are studied as a function of applied potential. It was assumed that these studies would help clarify the regularities of the formation of adsorption layers and estimate the prospects of modifying an SS surface in order to form protective polymeric films based on nitrogen- and sulfur-containing organic molecules.

Experimental

In this study we used recrystallized polyoxometalates, namely, phosphomolybdic acid $H_3PMo_{12}O_{40} \sim 15H_2O$ (PMo_{12}) and phosphotungstic acid $H_3PW_{12}O_{40} \sim 17H_2O$ (PW_{12}), Na_2MoO_4, as well as 1 N H_2SO_4. The POM structures are given in Fig. 1.

It is noteworthy that in acidic media, monomeric molybdate Na_2MoO_4 is substantially polymerized to give $Mo_7O_{24}^{6-}$ or $Mo_8O_{26}^{4-}$ [24]. An increase in acidity results in an increase in the number of molybdenum atoms in the polymer (up to 112 or more if reduction is carried out in acidic solutions) [25]. Mononuclear MoO_2^{2+} complexes should prevail in solutions with pH 0.9 or lower.

In electrochemical measurements, a three-electrode cell was used with an SS cylinder (0.8 cm in diameter) sealed in a Teflon holder as the working electrode. The samples were processed mechanically: first abraded using emery papers of various granularity, then polished with diamond powders to a mirror finish. After polishing, samples were degreased with acetone and repeatedly washed with distilled water.

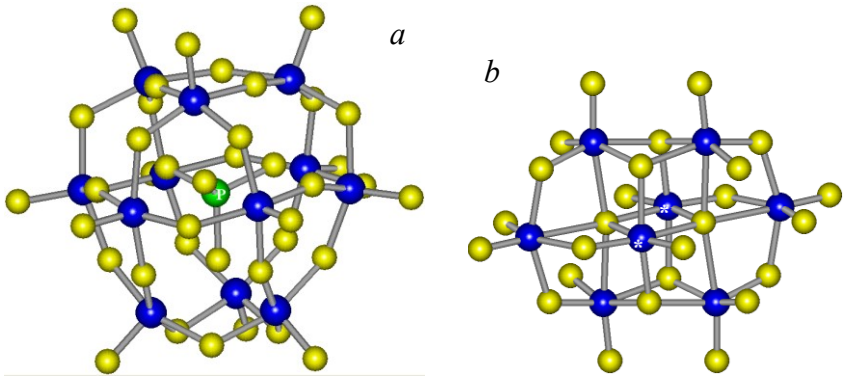

Fig. 1. Structures of $PMo_{12}O_{40}^{3-}$ (PMo_{12}) (*a*) and $Mo_8O_{26}^{4-}$ (*b*).

A platinum foil was used as the auxiliary electrode and a silver–silver chloride electrode was used as the reference one. Potentials were converted to the standard hydrogen scale (+200 mV).

Potentiodynamic curves were recorded with a PAR 173 potentiostat. The potential scan rate was set to 20 mV/min. All experiments were made in stirred working solutions without deaeration at ambient temperature (22±4°C). As appears from XPS analysis [26], such temperature variations practically do not affect both the thickness and composition of a passive film, though at smaller chromium concentrations in an alloy, an increase in temperature to 70°C results in some changes in the electrochemical properties and composition of the surface [27].

After polishing, the natural oxide layer was removed from the SS surface by depassivation of a sample in 1 N H_2SO_4 for 15 min at E = –450 mV. A new passive layer was then created on the surface of the sample by electrochemical polarization in the same solution at a preset potential (E_a) for 30 min. Then a POM under study was added to the solution with stirring and polarization at E_a was continued for 30 min. The stability of the oxide layers formed on SS samples under various conditions was estimated by time t required for depassivation of the sample after formation of a passive film and transfer of the sample into pure 1 N H_2SO_4.

XP spectra were recorded by means of a CLAM100 analyzer (50 eV) with an aluminum X-ray anode (200 W) attached to an HB100 Auger microscope (VG UK). The pressure in the analyzer did not exceed 10^{-8} Torr. The spectrometer was calibrated against the binding energies (E_b) of $Cu2p_{3/2}$ = 932.7 and $Au4f_{7/2}$ = 84.0 eV for copper and gold samples cleaned by argon ion sputtering. Samples for XPS studies were prepared in the same way as for the electrochemical tests. The binding energies E_b of electrons of the corresponding core shells of the atoms that constitute the surface were standardized by the C1s peak whose E_b was taken equal to 285.0 eV. For qualitative and quantitative analysis of the films formed on the surface, the following XPS lines were measured: Fe2p, Cr2p, O1s, C1s, Mo3d, W4f, and S2p. After exposure of samples to sulfuric acid, SO_4^{2-} anions are nearly always found in the surface layers. The S2s peak (for S^{6+}, E_b = 233.4 eV) is

superposed on the Mo3d spectrum (220–240 eV), therefore the area of the S2s peak whose intensity is determined from the S2s/S2p peak ratio should be subtracted from the intensity of the Mo3d doublet.

The integrated areas under the peaks are assessed after Shirley background subtraction [28]. The XP Fe2p spectrum and, to a slightly smaller extent, the Cr2p spectrum are considerably complicated by the presence of different oxidation states of iron and satellite peaks that can result in quantitative analysis errors [29–41]. To determine the contributions of oxide and metallic iron and chromium, the curve fitting method was used. Spectra of individual of iron and chromium oxides were measured and simulated by means of XPSPeak41 software [42]. XPS of the clean metals were obtained after ionic sputtering. The binding energies of the corresponding peaks well agree with the literature data [34–36, 43].

The thickness of each layer formed on the surface is determined using a MultiQuant program [44] in which the mean escape lengths of electrons calculated by the Cumpson and Seah formula [45] and the standard densities for iron and chromium oxides were used. The density of carbonaceous contamination is taken as 0.8–0.9 g/cm^3 [44], and those for PMo_{12} and PW_{12} are taken from published data [46, 47].

Results and discussion

Electrochemical behavior of SS in 1 N H_2SO_4. The potentiodynamic anodic curves of SS in 1 N H_2SO_4 solution without and with POMs in various concentrations appeared to be rather similar (as an example, the curves for solutions containing different quantities of molybdate are given in Fig. 2a). It is seen that in the acid without the additive, the initial current (~9 mA/cm^2) drops nearly to zero above the passivation potential (–171 mV) due to the formation of a passive film that is characteristic of stainless steels.

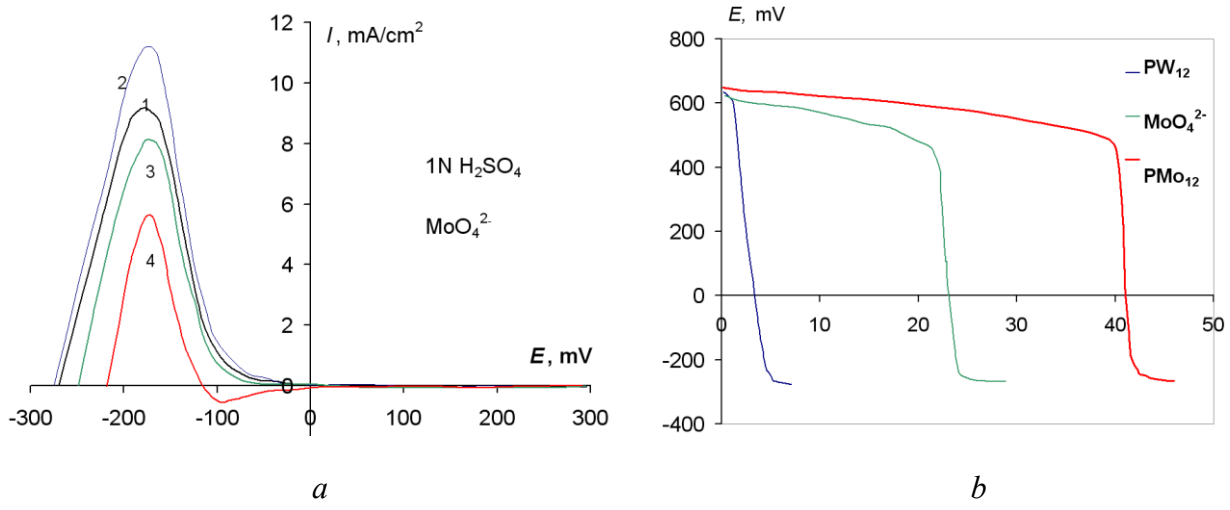

a *b*

Fig. 2. Potentiodynamic curves of SS in a 1 N H_2SO_4 solution without and with Na_2MoO_4 (*1* – 0; *2* – 3 g/l; *3* – 6 g/l; *4* – 9 g/l) (*a*); depassivation of SS in pure 1 N H_2SO_4 solution after the formation of a layer by electrochemical polarization at E = 700 mV in 1 N H_2SO_4 in the presence of the corresponding POM (*b*).

It is worthy of note that the current increase in the range from –300 to –100 mV is well consistent with the mass loss of SS in sulfuric acid in the same range of potentials [48]. As analysis of a solution after SS passivation shows, it is related to active dissolution of the alloy with release of Fe^{2+} cations into solution [49, 50].

The addition of a POM to the electrochemical cell was carried out at the free corrosion potential E_{st} = –(270–280) mV after preliminary depassivation of samples at –450 mV. After that, a positive shift of corrosion potential occurs (Table 1). Increasing the POM concentration is accompanied by a decrease in the active dissolution current of SS, and different quantities of POMs are needed to reduce the current density twofold.

Table 1. Steady-state potentials of 17Kh1T stainless steel in pure 1 N H_2SO_4 and in the presence of POMs.

Compound	*C*, g/l	E_{st}, mV *	E_{st}, mV **	E_{pas}, mV	I_{pas}, mA/cm^2
H_2SO_4	–	–275±10	–275±12	–171±10	9±2
PMo_{12}	6	682±10	–225±12	–156±10	4±2
Na_2MoO_4	9	470±20	–225±12	–171±10	5±2
PW_{12}	12	20±20	–245±12	–160±10	6±2

*With oxide layer; ** after cathodic depassivation.

Reduction in the limiting current of anodic dissolution with an increase in POM concentration is characteristic of passivation type inhibitors.

A specific feature of the behavior of an SS electrode in sulfuric acid without and with addives should be noted. The samples immersed in sulfuric acid immediately after polishing yield an instant potential of +670 mV, which drops to –270 mV at once (no more than in 1 min), whereas the samples kept for 24 h in the air require a longer time for that. However, upon exposure of samples after polishing and ageing for 24 hours, *i.e.*, after formation of a sufficiently thick passive film, in sulfuric acid with a POM additive, the electrode potential E_{st} first undergoes some negative shift and then shifts to the values specified in Table 1. The POM concentration should be above some critical value after which electrode passivation occurs.

To study the influence of POM addition on the protective properties of the passive layer formed on SS in 1 N H_2SO_4, the samples are preliminarily depassivated for 15 min in 1 N H_2SO_4 at E = –450 mV. Then, the potential is switched to the working potential, E_w. Potentiostatic polarization at E_w = +700 mV was carried out for 30 min, then a POM was added with stirring to the electrolytic cell in an amount required to reach the concentration specified in Table 1, and polarization was performed for 30 min. After that the polarization is discontinued, and the potential reached a steady value after a while (Table 1).

The passive film formed at +700 mV in 1 N H_2SO_4 in 2 hours is not preserved after polarization is switched off, because the electrode potential drops to the corrosion potential

practically at once. On the other hand, the films formed in the presence of PMo_{12} in 1 h acquire an after-effect, *e.g.*, E_{st} is maintained for 40–60 min after changing the working solution for pure 1 N H_2SO_4 (Fig. 2b).

Apparently, addition of PMo_{12} to sulfuric acid affects the electrochemical behavior of SS samples considerably. Naturally, there is a question whether the PMo_{12} anion (the anion diameter being ~1 nm) operates as a unit or decomposes into fragments that occupy the active sites on the surface and thus interfere with corrosion. Therefore, it was interesting to study the behavior of SS in the presence of MoO_4^{2-} which is known to form a POM at low pH [24] and which can be considered as a PMo_{12} fragment.

Immersing the sample after depassivation in the acid at E_w = +700 mV for 30 min followed by addition of Na_2MoO_4 (9 g/l) results in a stable film with E_{st} = +(470–480) mV. This value is lower than the E_{st} value reached in the presence of PMo_{12}. The protective after-effect of molybdate is also lower than that created by PMo_{12} (Fig. 2b).

Does the form of the PMo_{12} anion affect the coverage and blockage of the active sites in the surface layer, or do certain redox properties of molybdenum play a specific role? To clarify this question, the behavior of SS in the presence of PW_{12} was studied as its structure and size are identical to those of PMo_{12} (Fig. 1), but the half wave reduction potential is by ~0.4–0.5 V more negative than that of PMo_{12} [24].

It follows from the potentiodynamic curves on SS in 1 N H_2SO_4 containing PW_{12} that the anodic current density at PW_{12} concentration <9 g/l is notably higher than the maximum current in the absence of PW_{12}. A twofold reduction in the maximum current is observed at a PW_{12} concentration of 12 g/l that approximately corresponds to the molar concentration of PMo_{12}.

The influence of PW_{12} on SS stability in acid was studied at the concentration C = 12 g/l. The potential of an oxidized SS sample exposed for 24 hours in air after polishing got the value E_{st} = +280 mV. This value was retained for a few minutes and then decreased to E_c. The after-effect was maintained for 15–20 min (Fig. 2b).

Thus, after formation of an oxide layer of sufficient thickness as a result of POM influence, incorporation of these compounds in the oxide layer structure prevents its destruction by the acid, and the steady-state potential of the electrode depends on the critical POM concentration above which (except for PW_{12}) it remains unchanged. The change in the steady-state potential is caused by differences in the nature of effects on the electrochemical behavior of SS. Therefore, PMo_{12} anions are assumed to be built into the oxide layer without decomposition and the redox properties of PMo_{12} play an important role in creation of a stable oxide film.

XPS studies of SS surface after exposure to 1 N H_2SO_4 and in the presence of POM

In order to study the quantitative and qualitative composition of the surface layers formed on SS in 1 N H_2SO_4 without and in the presence of PMo_{12}, MoO_4^{2-} and PW_{12}, XP spectra of Fe2p, Cr2p, C1s, O1s, Mo3d, W4f, S2p electrons were recorded. Practically in all cases,

the spectra reveal some variation in intensity of the peaks caused by different states of elements. As an example, typical spectra and their components measured on the SS sample after exposure to 1 N H_2SO_4 in the presence of PMo_{12} at a potential of E_w = +700 mV and –50 mV are shown (Fig. 3).

The O1s spectrum can be decomposed into three peaks, which are routinely assigned to water molecules and hydroxy groups, as well as the oxygen atoms forming iron and chromium oxides. In the case of $Cr2p_{3/2}$ electrons, a basic doublet corresponding to CrOOH at 577.1±0.1 eV and a small shoulder at 564.4±0.2 eV which should be assigned to metallic chromium are observed most commonly. However, as it will be shown below, it can be assumed from analysis of angular resolved XPS that the Cr2p spectrum should consist of three doublets, as shown in Fig. 3b.

For all SS samples except those exposed at –40 mV, after separation of the doublet corresponding to Fe^0, it is possible to deconvolute the Fe2p spectrum into some doublets characteristic of Fe_3O_4 (710.2±0.2), Fe_2O_3 (711.2±0.2), and FeOOH (711.8±0.2 eV). However, as our experiment shows, the degree of the spectral resolution of peaks, unfortunately, does not allow us to deconvolute unequivocally a spectrum into different oxide components. As it appears from [38], even upon addition of three spectra corresponding to individual oxides and the metallic state, the E_b of Fe2p electrons should be displaced relative to the initial positions to make the simulated spectrum close to the experimental one.[1] Furthermore, for calculations we will use the total intensity of all oxides as, proceeding from our data, in any case the error in assessments of the contribution of metallic components does not exceed 10%. According to calculations, the atomic ratio $Cr_{ox}/Cr_{ox}+Fe_{ox}$ in a passive film is always larger than the chromium content in an alloy. It is observed nearly for all Fe–Cr alloys [51–56].

At the full passivation potential (–50 mV), the film composition varies essentially and two doublets are observed that correspond to completely oxidized iron, Fe_2O_3 (for $Fe2p_{3/2}$, E_b =711.4 eV), with its characteristic satellite doublet shifted by ~8 eV relative to the basic doublet (Fig. 3c) [34, 35].

The integrated intensity and position of XPS peaks for SS samples kept in 1 N H_2SO_4 were used to determine the atomic concentrations of iron and chromium and their oxides in the surface layer depending on the applied potential E_w (Fig. 4a). At negative potentials, the concentration of oxidized iron in the film differs only slightly from the Cr/Fe ratio in the alloy bulk. In the passive area, the ratio of chromium and iron remains nearly constant, which is consistent with published data [57]. For comparison, the anodic curve is superimposed on the plot of the atomic concentration measured at the applied potential (Fig. 4). As the results of isotope exchange of oxygen show, no additional oxidation of the passive film formed at anodic potentials occurs, though the cathodically reduced surface quickly oxidizes on air [58]. Our data also confirms that the composition and thickness are

[1] Other approaches to analysis of XPS spectra components are given in our paper: L. P. Kazansky, Yu. E. Pronin, and E. M. Sokolova, *Korroz.: Mater. Zashch.*, 2011, no. 2, 13.

invariable in the working potential range, and those observed changes can be considered as real. A similar conclusion was made on the basis of *in situ* ellipsometric measurements of passive films of Fe17Cr alloy in 0.5 M H_2SO_4 [59].

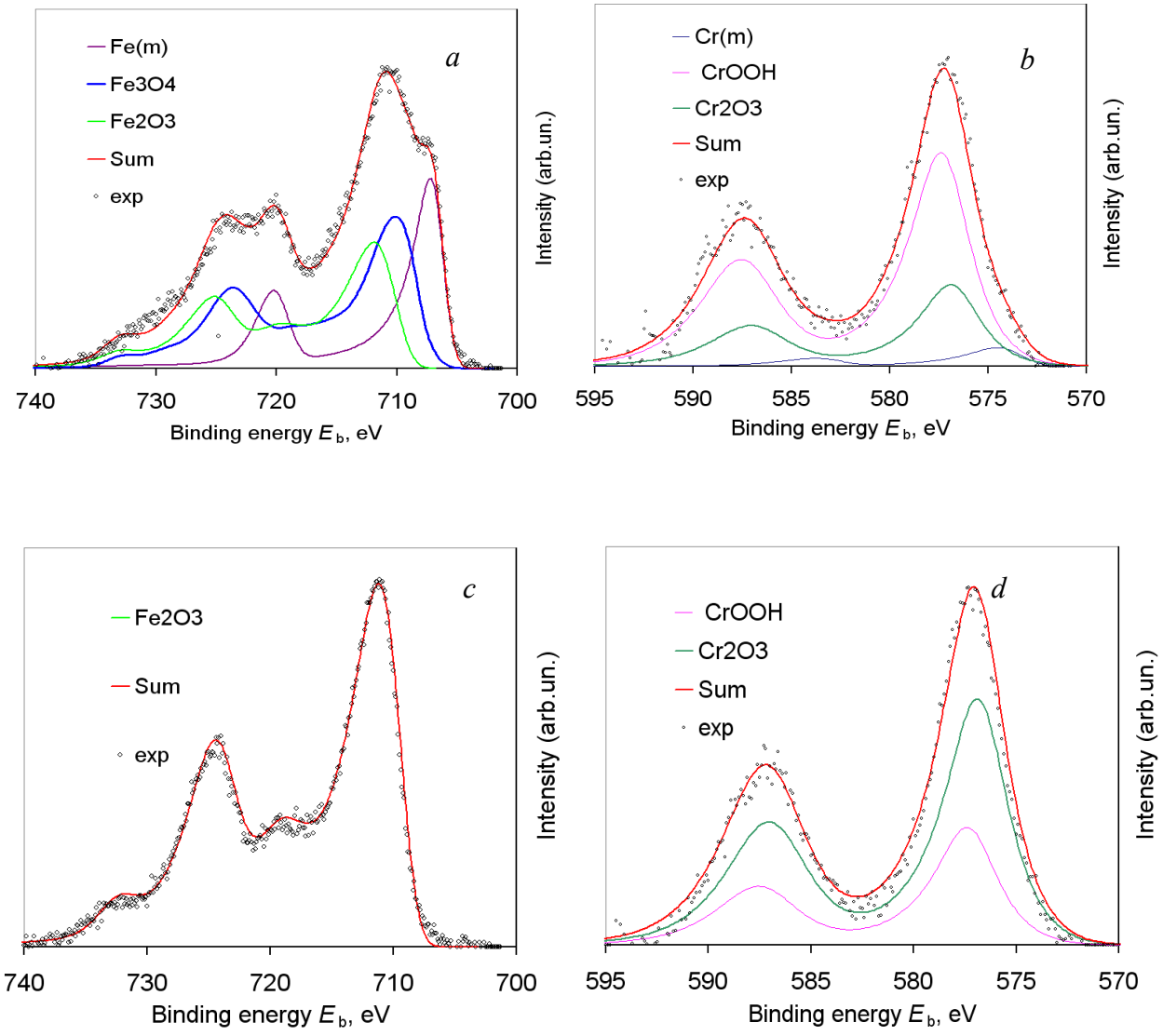

Fig. 3. XPS of Fe2p and Cr2p for SS samples after exposure to 1 N H_2SO_4 in the presence of PMo_{12} at E_w =+700 mV (*a* and *b*, respectively) and at –50 mV (*c* and *d*, respectively).

It is necessary to mention some feature of change in the Fe(ox)/Cr(ox) ratio at a point of the maximum anodic current at the passivation potential E_p = –150 mV. At this point, a maximum dissolution of iron occurs and consequently the concentration of chromium in the surface layer increases to 30%. Such change can at first be related to iron removal followed by chromium removal upon a slight positive shift of potential that corresponds to an increased content of iron in the surface layer. In some sense, this is consistent with two

the mass loss peaks in this range of potentials for Fe17Cr alloy obtained in corrosion experiments [48].

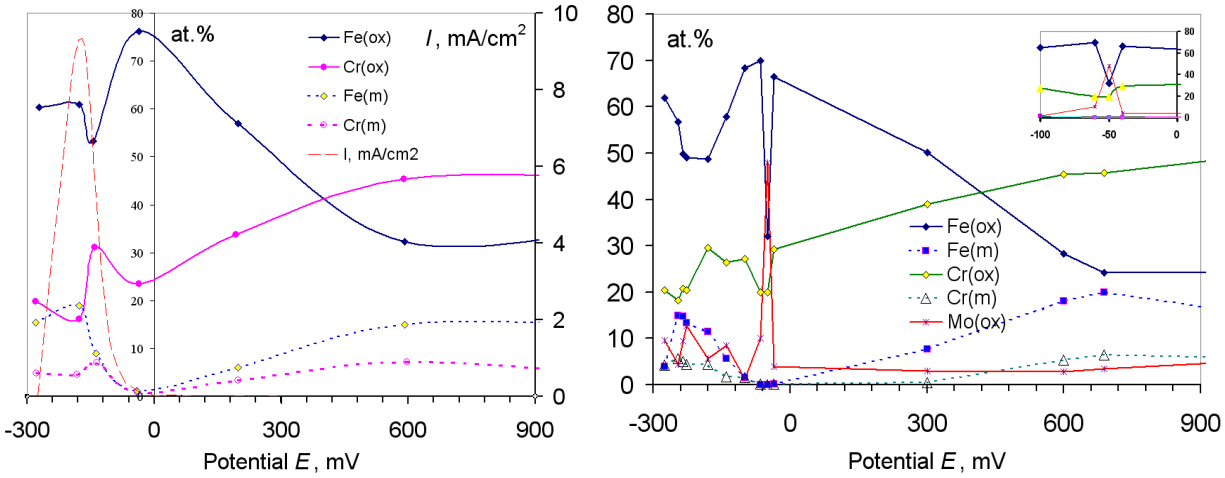

a *b*

Fig. 4. Composition of an oxide layer formed on SS surface depending on the applied potential in pure 1 N H_2SO_4 (*a*) and with addition of PMo_{12} (6 g/l) (*b*).

An increase in E_w from 0 V leads to a gradual increase in chromium content and a decrease in iron content in the oxide layer. As appears from the spectra, iron is present in the surface layer as Fe_3O_4, while chromium, according to the position of the $Cr2p_{3/2}$ peak, E_b = 577.2 eV, is mostly in the form of CrOOH, in agreement with literature data [39, 56].

The thickness of the layers formed at the working potentials was calculated from the integrated intensity of the corresponding peaks using Multiquant software. It was assumed that three layers exist on a sample surface: a topmost layer of carbonaceous contamination, a second hydroxyl layer, and then a layer of mixed oxides adjoining the surface. Each layer was assumed to be homogeneous in thickness and composition. It is also necessary to note the increased concentration of hydroxyl layer in the region of active film dissolution. The total thickness of the first and second layers can reach 3 nm.

Practically in all cases except at potentials in the range of ~0 to +100 mV (where the metal peak is not observed, *i.e.*, there is a thick oxide film), the thickness of the oxide layer does not exceed 1.5–2.5 nm. Oxides of approximately the same thickness are formed in acidic sulfate solutions in the presence of 0.3 M NaCl [60].

Naturally, the stratification of layers presented above does not correspond to real conditions where, first, there is no clear boundary between the layers, and, second, there is a heterogeneous distribution of iron and chromium in the oxide layer. The latter proves to be true, as it will be shown below, and is also confirmed by results of ionic scattering spectroscopy of oxide layers formed on a Fe–Cr alloy [61].

Similarly, changes in intensity ratio are observed for the elements in surface layers formed upon exposure of SS samples in 1 N H_2SO_4 containing 6 g/l of PMo_{12} (Fig. 4b). It

should be noted that at E_w = –50 mV (Fig. 4b, insert) there is a significant decrease in iron oxides and the surface layer is largely enriched with PMo_{12} anions. Above 0.0 V there is a gradual gain of chromium in the oxide and a decrease in iron oxide. In the anodic range of potentials, molybdenum is present basically as Mo^{6+} (E_b = 233.2 eV) and a small amount (no more than 15%) of its reduced form, Mo^{5+} (E_b = 232.2 eV). It is necessary to note that the P:Mo ratio in the top layer is close to that observed for crystalline PMo_{12} (1±0.3:12 Mo).

Similar results were observed in a study of Fe–Cr–Mo steel in hydrochloric acid [62] where at potentials around –150 mV the steel surface is considerably enriched with molybdenum at the expense of iron. However, in none of the cases were lower oxidation states of molybdenum observed. Sulfur, if observed, is present as SO_4^{2-} (for the S2p level, E_b = 169.3 eV). However, its partial transformation into S^0 is observed at negative electrode potentials.

Using the Multiquant program and integrated peak intensity of the corresponding elements, the formal thicknesses of layers were calculated under the assumption that a PMo_{12} layer is arranged on the mixed oxide layer or is incorporated in it. Comparison of the calculated and experimental relative peak intensities shows that the calculated thickness of PMo_{12} at E_w > 0 V does not exceed 0.2±0.1 nm, while the oxide layer thickness is 1.5–2.5 nm. It should be taken into account that the crystallographic diameter of the PMo_{12} and PW_{12} anions is ~1.1 nm [46, 47], hence, given the thickness of this calculated layer is 0.25 nm, the anions may form islets on the surface or be incorporated in the oxide film. The latter implies that $10\times10\times1$ nm^3 of the surface oxide layer can hold up to 25 PMo_{12} anions.

To elucidate the in-depth distribution of elements, angle resolved XPS and argon ion sputtering were undertaken on SS samples pretreated in sulfuric acid in the presence of PMo_{12} at +700 mV. In the first case, a simple approach was used [63]. To build the relative depth plot, XPS spectra were recorded at two angles of take-off photoelectrons – at the normal to the surface (so called "bulk angle") because the electrons travels from deeper layers than in a case of a "surface angle"–tilted trajectory of the photoelectrons (Fig. 5a). The $\ln I_s/I_b$ value, where I_s is the peak intensity of the atom under study measured at an angle of 55° and I_b is the peak intensity measured at normal take-off angle, may reflect the in-depth distribution of atoms in the surface layer. For larger $\ln I_s/I_b$ values, the atoms are arranged farther from the metal surface. According to the plot presented in Fig. 5a, molybdenum is in the upper layer.

A similar conclusion follows from the etching plot (Fig. 5b) showing that PMo_{12} anions are distributed in the top oxide layer. Sulfate anions are distributed throughout the oxide film. Results of etching shows a slight increase in the concentration of chromium oxide in the beginning, that evidences that the topmost layer is slightly enriched with iron oxide, which is consistent with a number of studies in acidic and neutral solutions [27, 33, 51, 61]. Besides, the $Cr2p_{3/2}$ peak is narrowed at a constant E_b = 577.3 eV, which specifies a decrease in the contribution of the Cr_2O_3 layer allocated closer to the alloy surface.

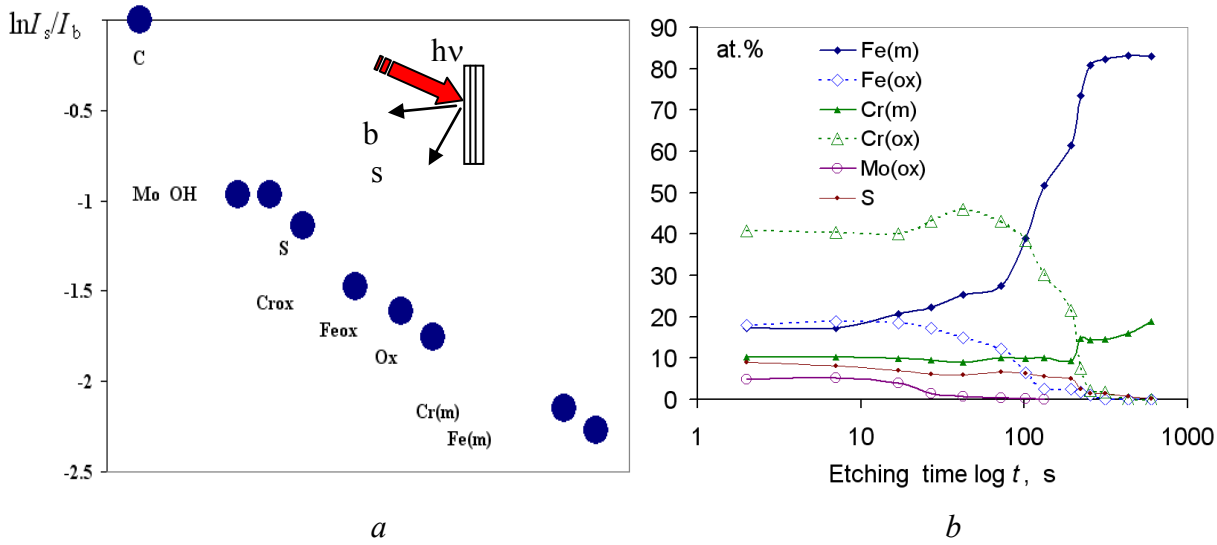

Fig. 5. Concentration dependence of metallic Fe, Cr, their oxides, sulfur and molybdenum depending on the angle of take-off electrons (*a*); concentration profile of the surface layer formed on SS sample exposed to 1 N H_2SO_4 containing 6 g/l of PMo_{12} at E_w = 700 mV (*b*).

Computation of concentration profiles of the surface layers obtained during argon ion sputtering was made on the assumption that there is no selective etching of iron or chromium, and also that during mild etching no reduction of oxides to the metallic state occurs, as follows from XPS analysis of the top layer formed on Fe–Cr alloys and on iron and chromium oxides [29, 64].

Considering the data of argon ion bombardment and angular dependence, one comes to a duplex model of the surface layer: a metal surface, on which primary mixed oxide layer Cr_2O_3 and Fe_3O_4 (thickness of 2.0±0.5 nm) is formed, on which a layer of CrOOH and iron oxide with impregnated PMo_{12} anions (1.0±0.5 nm) is allocated. A good agreement between the calculated and experimental dependences is obtained with the following ratio of the elements: 2Cr:0.3Fe and Mo:3Cr:6Fe for the first and second layers, respectively.

It is necessary to note that nanosized films and high reaction rates in surface layers do not allow better reproducibility of results to be attained for SS with 17% chromium. As 3D numerical modeling of the corrosion process of Fe-Cr alloys shows [65], passage from active dissolution to full passivation occurs in a narrow range of 16–19% of chromium and in this case the thickness and composition of the surface layer depend rather strongly on many factors that are difficult to control.

In the case of SS exposure to 1 N H_2SO_4 containing 9 g/l Na_2MoO_4, an increase in anodic potential results in an increase in the concentration of oxidized chromium (Fig. 6a). Similar changes are observed in the case of SS exposure to 1 N H_2SO_4 containing 12 g/l PW_{12} (Fig. 6b). In both cases, the $Fe2p_{3/2}$ peak due to metallic state is higher than the peak of oxidized iron, meaning that the oxide film is rather thin.

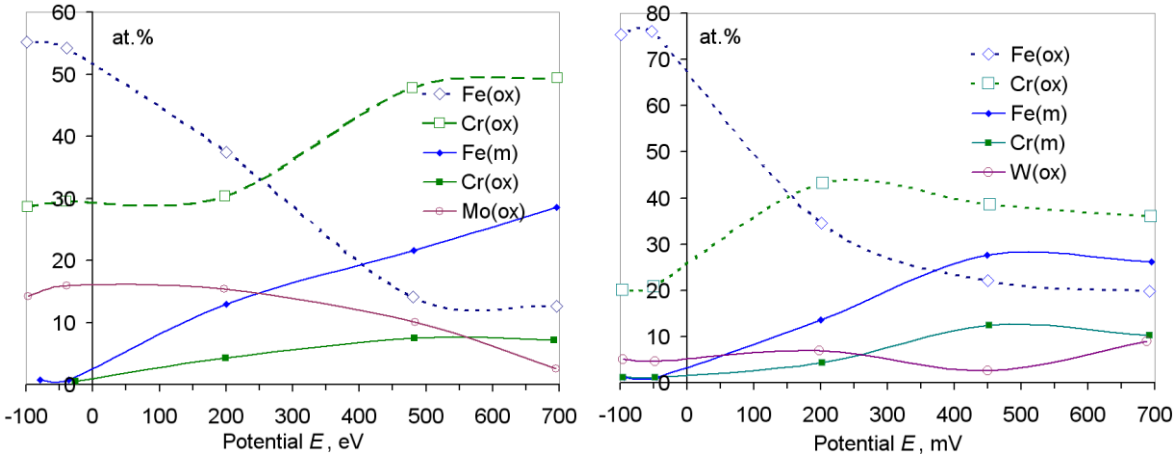

a *b*

Fig. 6 Atomic compositions of SS surface film after exposure in 1 N H_2SO_4 containing 9 g/l Na_2MoO_4 (*a*) and 12 g/l PW_{12} (*b*) depending on applied potential.

The effect of molybdenum as an alloying additive on the corrosion behavior of Fe–Cr steels was considered in a number of articles, for example in [62, 66–67]. It is considered that, on the one hand, molybdenum forms a protective MoO_2 film on the surface and reduces the active dissolution currents (for example by one order for Fe12Cr5Mo alloy [66] in 1 M H_2SO_4 or by 2 orders in the case of Fe30Cr2Mo steel in 1 M HCl [68]). Thus, molybdenum will neutralize active sites on the surface and favor the formation of homogeneous passive layers [69]. On the other hand, molybdenum increases the electronic conductivity of a passive top layer due to an increase in the degree of non-stoichiometry, resulting in acceleration of dissolution of iron from an alloy [66]. It is noteworthy that the molybdenum concentration in a steel oxide surface layer in the passive region [69] is comparable to that achieved in the presence of PMo_{12} and MoO_4^{2-}. However, taking into account that an increase in PMo_{12} concentration in a solution does not result in a significant decrease in passivation currents, it is possible to assume that the passivation mechanism in this case is different from that characteristic of Fe–Cr–Mo alloys.

SS with tungsten as an alloying element have been studied to a lesser degree and it is assumed that its difference from molybdenum is determined by the stability of the hexavalent oxide [52].

At high anodic potentials, because of a smaller oxidizing ability of polymolybdate and PW_{12}, iron oxidation occurs to a smaller degree than with PMo_{12}. This results in thinner films whose passivating properties are lower though they are incorporated in the oxide layer. During adsorption of PMo_{12} on the surface, 2 or 4 atoms of molybdenum are reduced to Mo^{5+}, thus increasing the negative charge of the anion from –3 to –5 or –7 that results in protonation of the PMo_{12} anion. This effect favors PMo_{12} retention in the oxide layer due to hydrogen bonds and creation of a thicker oxide layer; furthermore, such a nanosize film possesses an after-effect.

Conclusions

1) Immersion of a polished SS sample after a 24 h exposure in air into 1 N H_2SO_4, containing a critical concentration of a POM results in the establishment of steady-state potential specified in Table 1. In the case of PMo_{12} and molybdate, it remains constant for at least 2 h. In the case of PW_{12}, this potential is maintained for no more than 30 min and then it decreases to E_c.
2) Exposure of an SS sample at a potential of +700 mV for 30 min, addition of POM, and subsequent exposure for 30 min results in formation of a film possessing an after-effect. The film created in such a way is depassivated in pure 1 N H_2SO_4 in 40–60 min in the case of PMo_{12}, and 15–20 min in the case of molybdate, and more quickly for PW_{12}.
3) In all cases, the surface of an SS electrode kept at –50 mV in 1 N H_2SO_4 consists of a thick oxide. In the presence of POM, it is considerably enriched by Mo^{6+}. In the case of PMo_{12} the oxide layer thickness reaches >3 nm, while it is much thinner in the case of molybdate and PW_{12}. At positive potentials the oxide film enriched by Cr^{3+} is notably thinner, but nevertheless contains POMs in all cases.
4) In comparison with other POMs, the higher efficiency of PMo_{12} is presumably due to a larger oxidizing ability favoring the oxide growth, and a stronger ability to be retained in a top layer due to hydrogen bridges.

References

1. I. L. Rozenfel´d, *Ingibitory korrozii (Corrosion inhibitors)*, 1977, Moscow, Khimiya (in Russian).
2. J. P. G. Farr and J. Saremi, *Surf. Tech.,* 1982, **19**, 137.
3. D. M. Drazic and C. S. Hao, *Corros. Sci.*, 1983, **23**, 683.
4. Yu. N. Mikhailovsky, *Zashch. Met.*, 1984, **20**, 179 (in Russian).
5. R. M. Saleh, M. M. Badran, A. A. El Hozary and H. A. El Dahan, *Br. Corros. J.*, 1988, **34**, 1913.
6. S. Maximovich, G. Barral, F. Le Gras and F. Claudet, *Corros. Sci.*, 1995, **37**, 271.
7. G. X. Mu, Q. Qu and J. Zhou, *Corros. Sci.,* 2006, **48**, 445.
8. H. Konno, K. Narumi and H. Habazaki, *Corros. Sci.*, 2002, **44**, 1889.
9. K. Ogura and T. Ohama, *Corrosion (NACE)*,1984, **40**, no. 2, 47.
10. I. L. Rozenfeld, L. P. Kazanskiy, A. G. Akimov and L. V. Frolova, *Zashch. Met.*, 1979, **15**, 349 (in Russian).
11. D. V. Brasher and J. E. Rhoades-Brown, *Brit. Corros. J.*, 1969, **4**, 74.
12. E. A. Lizlovs, *J. Electrochem. Soc.*, 1967, 117, 1015.
13. L. V. Tumurova and L. P. Kazanskiy, *Izv. AN SSSR. Ser. khim.*, 1984, no. 9, 1947.
14. L. V. Tumurova, E. V. Kvashnina, L. P. Kazanskiy and M. V. Mohosoev, *Zashch. Met.*, 1990, **26**, 942 (in Russian).
15. A. J. Pikelniy, G. G. Reznikova, A. P. Brynza, S. A. Khmelovskaja and O. A. Pikelnaya, *Elektrokhimiya,* 1995, **31**, 529 (in Russian).

16. S. V. Lomakina, T. S. Shatova and L.P. Kazansky, *Corros. Sci.*, 1994, **36**, 1645.
17. M. Ge, B. Zhong, W. G. Klemperer and A. A. Gewirth, *J. Am. Chem. Soc*., 1996, **118**, 5812.
18. B. Keïta and L. Nadjo, *Surf. Sci. Lett*., 1991, **254**, L443.
19. B. A. Watson, M. A. Barteau, L. Haggerty, A. M. Lenhoff and R. S. Weber, *Langmuir*, 1992, **8**, 1145.
20. B. Keïta, F. Chauveau, F. Théobald, D. Bélanger and L. Nadjo, *Surf. Sci.*, 1992, **264**, 271.
21. N. Mizuno and M. Misono, *Chem Rev*., 1998, **98**, 199.
22. A. Rothschild, C. Debiemme-Chouvy and A. Etcheberry, *Appl. Surf. Sci*., 1998, **135**, 65.
23. D. E. Katsulis, *Chem. Rev.*, 1998, **98**, 219.
24. M. T. Pope, *Heteropoly and Isopoly Oxometalates*, Springer-Verlag Berlin, 1983.
25. A. Müller, E. Beckmann, H. Bögge, M. Schmidtmann and A. Dress, *Angew. Chem.*, 2002, **114**, 1210.
26. S. Jin and A. Atrens, *Appl. Phys.*, 1988, **A45**, 83.
27. N. DeCristofaro, M. Piantini and N. Zacchetti, *Corrosion Sci.*, 1997, **39**, 2181.
28. D. A. Shirley, *Phys. Rev*., 1972, **B5**, 4709.
29. S. Mischler, H. J. Mathieu and D. Landolt, *Surf. Interface Anal.*, 1988, **11**, 182.
30. T. C. Lin, G. Sesadri and J. A. Keller, *Appl. Surf. Sci*., 1997, **119**, 83.
31. P. Brüesch, K. Müller, A. Atrens and H. Neff, *Appl. Phys.*, 1985, **A38**, 1.
32. C. Hubschmid, D. Landolt and H. J. Mathieu, *Fresenius J. Anal. Chem.*, 1995, **353**, 234.
33. J. E. Castle, H. Chapman-Kpodo, A. Proctor and A. M. Salvi, *J. Electron Spectr. Rel. Phen.*, 2000, **106**, 65.
34. P. C. J. Graat and M. A. J. Somers, *Appl. Surf. Sci*., 1996, **100/101**, 36.
35. M. Aronniemi, J. Sainio and J. Lahtinen, *Surf. Sci*., 2005, **78**, 10.
36. A. M. Salvi, J. E. Castle, J. F. Watts and E. Deimoni, *Appl. Surf. Sci*., 1995, **90**, 333.
37. C. J. Powell and J. M. Conny, *Surf. Interface Anal*., 2009, **41**, 804.
38. A. P. Grosvernor, B. A. Kobe, N. S. McIntyre, S. Tougaard and W. N. Lennard, *Surf. Interface Anal*., 2004, **36**, 532.
39. T. Y. Yamamura, N. Okuyama, Y. Shiokawa, M. Oku, H. Tomiyasu and W. Segiyama, *J. Elecrochem. Soc*., 2005, **152**, B540.
40. K. Asami, K. Hashimoto and S. Schimodaira, *Corros. Sci*., 1977, **17**, 713.
41. V. Maurice, W. P. Yang and P. Marcus, *J. Electrochem. Soc*., 1996, **143**, 1182.
42. XPS Peak4.1 © Kwok R.W.M. email: rmkwok@cuhk.edu.hk
43. C. D. Wagner, C. J. Powell, J. W. Allison and J. R. Rumble, *NIST X-ray Photoelectron spectroscopy Database (Version 2.0)*, National Institute of Standards and Technology, Gaithersburg, MD, 1997.
44. M. Mohai, *Surf. Interface Anal.*, 2004, **36**, 828.
45. P. J. Cumpson and M. P. Seah, *Surf. Interface Anal.*, **25**, 430.
46. H. D'Amour and R. Allman, *Z. Krist.*, 1976, **143**, 1.

47. G. M. Brown, M. R. Noe-Spirlet, W. R. Busing and H. A. Levy, *Acta Crystallogr.*, 1977, **B33**, 1038.
48. V. P. Razygraev, M. V. Lebedeva, E. Yu. Ponomareva and V. I. Spitsyn, *Dokl. AN SSSR*, 1987, **294**, 642 (in Russian).
49. J. E. Castle and J. H. Qiu, *Corros. Sci.*, 1989, **29**, 91.
50. D. Hamm, K. Ogle, C.-O. A. Olsson, S. Weber and D. Landolt, *Corros. Sci.*, 2002, **44**, 1443.
51. I. Marcus, *Corros. Sci*., 1988, **28**, 589.
52. C.-O. A. Olsson and D. Landolt, *Electrochimica Acta*, 2003, **48**, 1093.
53. S. Haupt and H.-H. Strehblow, *Corros. Sci*., 1995, **37**, 43.
54. C.-O. A. Olsson, P. Agarwala, M. Freyb and D. Landolt, *Corros. Sci*., 2000, **42**, 1197.
55. *Corrosion Mechanisms in Theory and Practice*, 2002, ed. Marcus, Marcel Dekker, Inc.
56. R. Kirchheim, B. Heine, H. Fischmeister, S. Hofmann, H. Knote and U. Stolz, *Corros. Sci.*, 1989, **29**, 899.
57. B. S. Norgren, M. A. J. Somers and J. H. W. deWit, *Surf. Interface Anal.*, 1994, **21**, 378.
58. C. Courty, H. J. Mathieu and D. Landolt, *Electrochim. Acta*, 1991, **36**, 1623.
59. L. C. Jacobs, H. De Vogel, K. Hemmes, M. M. Wind, J. H. W. De Wit, *Corros. Sci.*, 1995, **37**, 1211.
60. W. Yang, D. Costa and P. Marcus, *J. Electrochem. Soc.*, 1994, **141**, 2669.
61. C. Calinski and H.-H. Strehblow, *J. Electrochem. Soc.*, 1989, **136**, 1328.
62. K. Hashimoto, K. Asami and K. Teramoto, *Corros. Sci*., 1979, **19**, 3.
63. A. Herrera-Gomez, J. T. Grant, P. Cumpson, M. Jenko, F. S. Aguirre-Tostado, C. R. Brundle, T. Conard, G. Conti, C. S. Fadley, J. Fulghum, K. Kobayashi, L. Kover, H. Nohira, R. L. Opila, S. Oswald, R. W. Paynter, R. M. Wallace, W. S. M. Werner and J. Wolstenholme, *Surf. Interface Anal.*, 2009, **41**, 840.
64. R. L. Tapping, R. D. Davidson and T. E. Jackman, *Surf. Interface. Anal.,* 1985, **7**, 105.
65. B. Diawara, M. Legrand, J.-J. Legendre and P. Marcus, *J. Electrochem. Soc.*, 2004, **151**, B172.
66. M. Bojinov, G. Fabricius, T. Laitinen, K. Mäkelä, T. Saario and G. Sundholm, *Electrochim. Acta*, 2001, **46**, 1339.
67. A. Greeff, C. W. Louw and H. C. Swart, *Corros. Sci.*, 2000, **42**, 1725.
68. K. Hashimoto, K. Asami, A. Kawashima, H. Habazaki and E. Akiyama, *Corros. Sci*., 2007, **49**, 42.
69. M.-W. Tan, E. Akiyama, H. Habazaki, A. Kawashima, K. Asami and K. Hashimoto, *Corros. Sci.*, 1997, **39**, 589.

♦ ♦ ♦